

Visualisation and Analysis of Polyethylene Coextrusion Melt Flow

Mike T. Martyn^a, Phil D. Coates^a and Martin Zatloukal^b

^a*IRC in Polymer Science & Technology, School of Engineering, Design & Technology
University of Bradford, Bradford BD7 1DP, UK.*

^b*Polymer Centre, Faculty of Technology, Tomas Bata University in Zlín,
TGM 275, Zlín, Czech Republic.*

Abstract. Polymer melts experience complex, time variant, stress and deformation fields on their passage through fixed geometries in many conversion operations. Flow complexity is further increased in operations involving the co-joining of two or more melt streams where one confining boundary is moving and viscoelastic. Such a complex situation arises in coextrusion processes. This work covers experimental studies on polyethylene melt flows in complex coextrusion geometries with a view to understanding the stress fields involved and their effects on flow stability.

A 30° coextrusion geometry is studied using two extrusion arrangements. In one arrangement a single extruder is used to feed a 'bifurcated' die design wherein the melt stream is split prior to, and rejoined after, a divider plate in the die. In the other design melt streams are delivered to, and converged at 30°, using two independent extruders. In a second die melt streams are brought together at 90°. In each die arrangement melt flow in the confluent region and die land to the die exit was observed through side windows of a visualisation cell. Velocity ratios of the two melt streams were varied and layer thickness ratios producing instability are determined for each melt for a variety of flow conditions. Stress and velocity fields in the coextrusion arrangements were quantified using stress birefringence and particle image velocimetry techniques.

The study demonstrates conclusively that wave type interfacial instability occurred in the coextrusion geometries when the same low density polyethylene melt is used in each stream. This observation occurred at specific, repeatable, stream layer ratios in each die arrangement. The complex flows were numerical modelled using a modified Leonov model and Flow 2000™ software. There was reasonable agreement between modelled at experimentally determined stress fields. Modelling however provided far more detailed stress gradient information than could be resolved from the optical techniques. A total normal stress difference (TNSD) sign criterion was used to predict the critical layer ratio for the onset of the interfacial instability in one die arrangement and good agreement between theory and experiment has been obtained.

The study conclusively demonstrates wave type interfacial instability in the coextrusion process is not caused by process perturbations potentially introduced by extruder screw rotation but is associated with process-history dependant differences in melt elasticity.

Keywords: Coextrusion, Instability, Imaging, Modeling.

PACS: 47.11.Fg, 47.20.Gv, 47.20.Ma, 47.50.Gj, 83.50.Ha, 83.50.Uv, 83.60.Wc, 83.80.Sg, 83.85.Ei

INTRODUCTION

In the extrusion of polyethylenes through capillary and film dies processors often experience a transition to a surface distortion known as "sharkskin" at critical stresses that are typically of the order of the plateau modulus. Sharkskin is characterized by high-frequency, small-amplitude surface distortions with one or more well-defined dominant wave numbers. At a second critical stress there is an apparent discontinuity in the flow curve, with the transition characterized in a constant throughput experiment by oscillating pressures and alternately smooth and shark skinned extrudates (known as "slip stick"). At progressively higher extrusion rates the extrudate becomes grossly distorted and has the appearance of being fractured. The instabilities described, and covered more completely in other works [1-4] are associated with polyethylene flow through 'fixed' boundaries: the metal die walls, where melt flow is rigidly constrained by the metal die walls.

But what about more complex flow systems where one boundary is moving, and indeed where the moving boundary is viscoelastic. Such a situation occurs in melt coextrusion processes. The moving interface between two melt streams forms one of the boundaries constraining flow of the melts.

Understanding mechanisms associated with the instability of interfaces in multilayer melt flow is the topic of this paper. An interface is always formed between adjacent viscoelastic melts in multilayer flows and this can exhibit instability. There are distinct types of 'interfacial instability' associated with the unsteady-state distortion of the interface of co-joining melt streams. Two types of interfacial instability dominate coextrusion flow with each type having peculiar characteristics. The first type is categorised as 'zig-zag instability' and is visually recognisable by a high periodicity, low amplitude, patterning of the melt re-arrangement at the interface. The second type of interfacial instability is termed 'wave instability' which has low periodicity and relatively high amplitude disturbance of the interface. In both cases the interface disturbance does not necessarily propagate to the surface of extrudate, it can simply appear as internal patterning, of parabolic form, of the stratified structure. Interfacial instability is detrimental to process output.

The coextrusion process has been the subject of many experimental and numerical studies [5-16] over the past three decades. Such studies have been conducted to enhance our fundamental understanding of the mechanisms and kinematics involved in bringing together several melt streams with different rheological properties and temperature fields. Such differences in the melt stream properties can lead, under certain processing conditions, to interfacial instabilities which limit production output or lead to poor product quality. Studies of flow instability are therefore of prime interest to processors.

In previous studies [17-20] we have successfully developed and applied flow visualisation and image analysis techniques to quantify layer ratio and velocity conditions promoting wave type interfacial instability in the coextrusion of the same LDPE melt. The work has demonstrated a strong correlation between layer ratio and interfacial instability. Additionally the studies suggest the wave instability is initiated in the confluent region of the coextrusion die. The work reported here builds upon our previous research and understanding of the mechanism(s) promoting interfacial

instability in polymer processing. The results of our experimental approach should, ultimately, provide a set of guidelines to enable accurate modelling and prediction of instabilities in coextrusion flows.

EXPERIMENTAL

Two low density polyethylene (LDPE) polymers commonly used in film production are used in this study. These were grade LD150R (Dow Chemicals) and Lupolen 1840H (Basell) polyethylenes. Salient characteristics of these polymers are provided in Table 1. The viscoelastic properties of these melts were measured using an Advanced Rheometric Expansion System (ARES 2000) rheometer with 25 mm diameter parallel plate geometry. The melts were assessed at various temperatures in a nitrogen atmosphere. The frequency sweep of the dynamic moduli G' and G'' were determined in a linear viscoelastic response range of strain independent data. The time-temperature superposition dynamic shear moduli and the shear and extensional properties of these polymers are reported elsewhere [21-22]. The LD150R melt was processed using set extruder barrel and die temperatures of 200°C and the Lupolen 1840H was processed at 150°C and 180°C.

TABLE 1. Characteristics of the low density polyethylenes evaluated.

<i>Polymer</i>	MFI* (g/10mins)	Density (kg/m³)*	SOC x 10⁻⁹ (m²/N)
Lupolen 1840H	1.5	919	1.34❖
Dow LD150R	0.24	916	2.19 ^u

* ASTM 1238 ■ ISO 1872/1 ^uat 200°C ❖ at 180°C

Flow cells on the dies enable melt flow in the confluent and die land regions to be observed. Image analysis is used to quantify the flow in these regions. The flow cells used in this study are reported in the following sections.

Extrusion Arrangement - 1

In the first arrangement only a single Davis Standard BC38 single screw extruder is used. The extruder was fitted with a modular die to take inserts to confer different convergence angles on co-joining melt streams. The melt passes from the extruder barrel into the die where it is subsequently split by a divider plate and rejoined at either 30° or 90° to form coextruded layers. A picture to the 30° geometry modular die is shown in Figure 1. Further details of the die and arrangement are given elsewhere [17-20]. The die has moveable restriction plates fitted in both streams which provide a means of altering the velocity ratios, hence stream thickness, at a given flow rate.

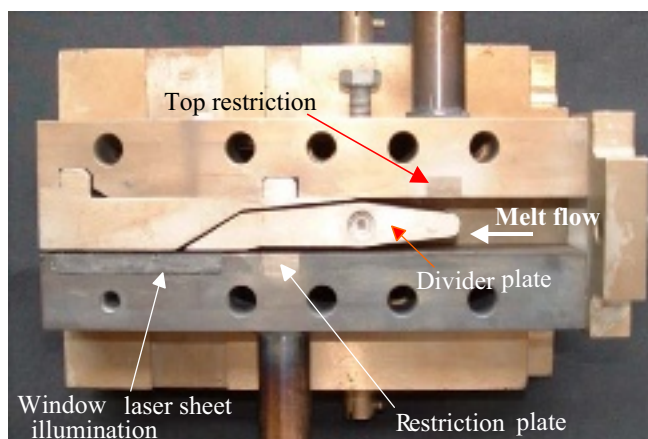


FIGURE 1. Photographs showing the internal channels of the flow visualisation cells.

Since melt is fed from the same extruder in this arrangement it is not possible to alter the stream velocities independently of the relative stream layer thickness. This is a limitation of the arrangement since it does not allow us to fully explore the contribution side stream velocity (hence melt stretching), has on interfacial instability using a single insert. It was possible to explore the effect of side stream velocity on interfacial stability by using another insert with a different side stream height.

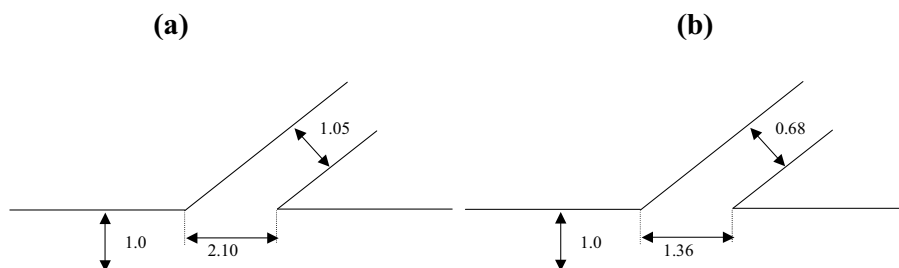


FIGURE 2. Schematics of the internal channels dimensions of the 30° geometry flow visualisation cells. Dimensions in mm. (a) 1.05 mm side channel, (b) 0.68 mm side channel.

Two 30° confluent geometries were therefore used to investigate the influence of side stream velocity. One insert was manufactured with a side stream height of 1.05 mm and the other with a side stream height of 0.68 mm. These geometries are shown schematically in Figure 2. A further die with a 90° confluence geometry of 0.83 mm fixed side stream height was also studied. In studies of flow in the both 30° and 90° confluent geometries the extruder screw speed was set to produce a constant flow rate of 1.36 (± 0.04) g/min for the LDPE melts through the die.

Extrusion Arrangement - 2

Two Davis Standard BC38 single screw extruders were used in the second coextrusion arrangement. The extruders are placed opposing each other. The extruders were independently controlled and fitted with general purpose 4:1 compression screws. Each extruder fed polymer melt stream into a modular flow cell with a 30° confluent geometry. The die and barrel were set at 200°C. A picture of the arrangement and modular die is shown in Figure 3. This arrangement enabled control of velocity of the individual polymer streams. The die also incorporates bleed ports in each stream. Opening the ports allows melt to by-pass the die enabling realistic melt histories (extrusion rates and melt residence times) to be achieved without over pressure of the flow cell. The height of both side and parallel channels in the confluent insert was 1.5 mm. Increase in channel height to 1.5 mm improved the visual resolution of stress birefringence patterns. The width of the channels was 25 mm. The die land length from the merging point to the slit end is set at 22.5 mm.

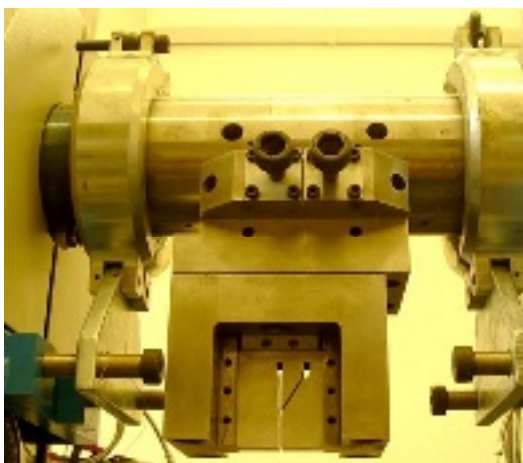


FIGURE 3. Pictures of the two stream die geometry and its arrangement on the Davis Standard BC38 extruders.

Initial studies are performed using the same LDPE melt, either Dow or Lupolen, melt in both streams. Further studies were then performed using the Dow and Lupolen melts in the separate coextrusion streams.

Process Measurement, Imaging Analysis and Modelling

Melt pressures were measured using Dynisco PT 422 1.5M pressure transducers in the dies. The screw speed of the extruders in each arrangement was monitored using an encoder on the drive of the screw. Pressure, screw speed and die temperature were monitored using a National Instruments A-D card and LabView programs developed in-house.

A darkfield, fieldwise, technique was used to view stress birefringence in the polymer melt flow in each arrangement. Stresses in the melt stream convergence region were quantified from birefringence patterns using the stress optical law and previously determined stress optical coefficients for the LDPE melt.

Digital image processing techniques were used to quantify the flow and instability. The reader is referred to previous reports of our studies [17, 18, 22] for greater detail of the optical and imaging system used. Digital processing of captured video enabled quantification of instabilities, birefringence patterns and velocity fields.

Velocity fields in the single fed die were measured using particle tracking velocimetry (PTV). The technique involved laser sheet lighting at a mid-plane in the die. A 0.5 %w addition of Ballontini glass particles (~40 to 70 μm and 2.50 sg) were introduced into the melt to act as tracers. The interface position and layer thickness ratio were also obtained by tracking the flow path of individual particles breaking from the apex of the divider plate into the main stream and the die land. The interface position in the two extruder arrangement was determined by using a low concentration of pigment in one of the streams.

A multi-step procedure was used in the simulation of the coextrusion geometry. Isothermal steady, two-dimensional, viscoelastic, finite element simulations were performed by solving mass, momentum and energy conservation equations using commercially available Flow 2000TM software package (Compuplast International Inc.). A modified White-Metzner constitutive equation, according to Barnes et. al. [23], is employed since this model shows close agreement with experimental data of steady shear and extensional viscosities of both LDPE melts with a single relaxation mode [21]. Knowledge of the normal stresses developed in the streams is required in order to calculate the relative stretching of the coextruded layers across the interface in the confluent region. Unfortunately the White-Metzner model fails to represent first normal stress difference properly. A modified Leonov model is therefore employed as a stress calculator. This constitutive equation is based on heuristic thermodynamic arguments resulting from the theory of rubber elasticity. With the aim to quantify the relative stretching of coextruded layers across the interface in the merging area, the *TNSD* (total normal stress difference) variable has been utilized. The normal stresses are calculated for two equivalent areas either side of the interface. The stresses in these two regions were consequently transformed into the local interface coordinate system and *TNSD* variable has been calculated as follows:

$$TNSD = N_{1,1} - N_{1,2} \tag{1}$$

where $N_{1,1}$ and $N_{1,2}$ represents the mean value of the first normal stress difference, in the flow area 1 in the major layer and flow area 2 in the minor layer, respectively, calculated over all chosen streamlines. More comprehensive details of the process are given in references [24, 25].

RESULTS AND DISCUSSION

Flow Analysis in Single Extruder Arrangement 1

30° Die Geometries

Data comparing conditions promoting stable flow and wave type interfacial instability for both melts in the 30° geometry are presented in Figure 4. Data includes measured pressure for Lupolen 1840H when processed at a flow rate of 1.38 g.min⁻¹ and temperature of 150°C. It should be noted that wave type interfacial instability occurred even though it was the same melt in both streams. We note the extrusion pressure is lower for the Lupolen at 130°C, reflecting the reduced viscosity of this melt compared with the Dow LD150R melt at comparable mass flow rates.

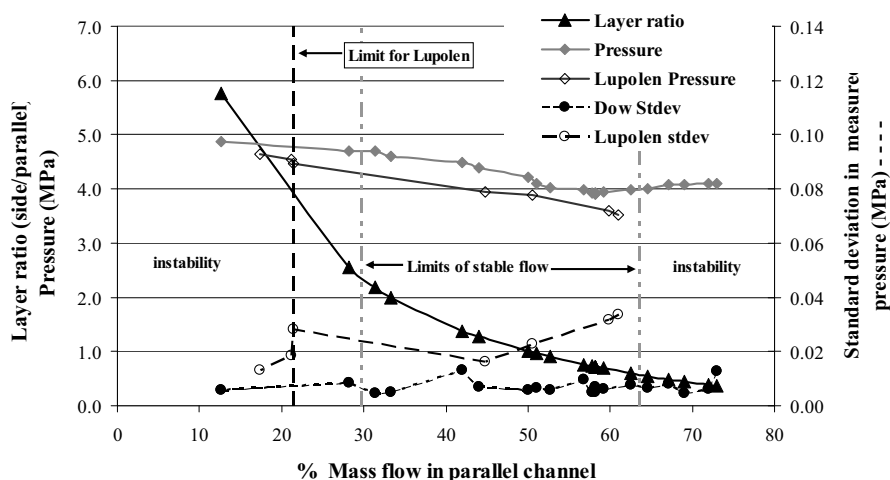


FIGURE 4. Measured pressure and limits of stable processing when melts are processed through the bifurcated melt coextrusion geometry. Dow LD150R (filled symbols) at 200°C and flow rate of 1.34 g/min. Lupolen (open symbols) at 150°C and flow rate of 1.38 g/min.

Vertical lines on Figure 4 demark regions of stable/unstable flow. Comparing the stabilities of the Dow LD150R and Lupolen melts at the respective processing temperatures, it is found the Lupolen melt can tolerate a greater difference in layer ratio before the onset of interfacial instability, i.e. a side/parallel layer ratio > 3.66:1 is required before interfacial instability occurs. Data given elsewhere [22] show there are differences in the elasticity of the melts with the Dow LD150R being the more elastic melt.

The Lupolen melt was also processed at a flow rate of $1.8 \text{ g}\cdot\text{min}^{-1}$ and a higher melt temperature of 180°C . Despite the increased flow rate no interfacial instability occurred at this temperature. From the dynamic data [21, 22] it is clear that Lupolen is less elastic than the Dow LD150R at the respective processing temperatures. The elastic modulus, G' , of Lupolen melt also reduces significantly with increase in temperature from 150°C to 180°C . A comparison of the process stability limits of Dow LD150R with those of the Lupolen, and noting the effects of temperature on the Lupolen stability, would suggest that interfacial instability is more likely to occur with increase in elasticity of the melt.

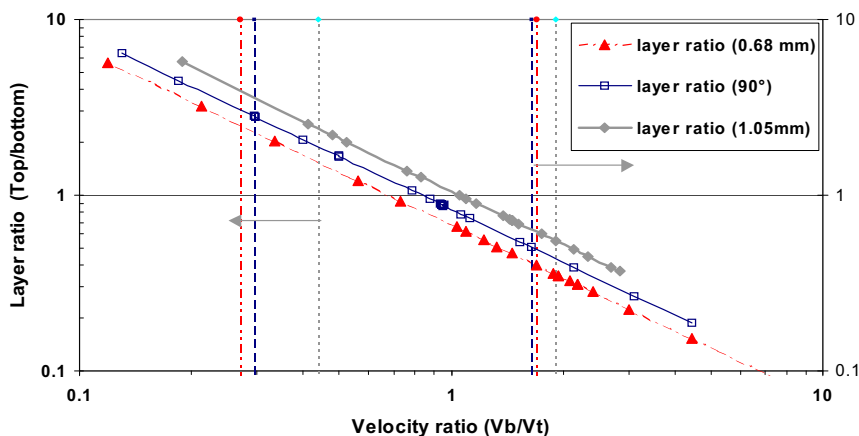


FIGURE 5. Influence of side channel height on flow stability. Regions defined by left and right arrows are unstable. Open symbols are 90° die geometry data.

Results of studies on the effect of channel dimension on stability are summarised in Figure 5. For purpose of clarity data is confined to studies on the Dow LD150R at 200°C . Regions to the left and right of the demarcation lines in the graph, defined by the arrows, are process conditions under which wave type instability occurred. The intermediate area defines conditions of stable flow, i.e. stable ‘processing window’. Comparing the layer ratio limits associated with stable processing it is clear stable flow conditions are promoted when side stream height is reduced. The geometry with the 0.68 mm side stream height can tolerate a greater difference in stream velocity and layer ratio before the onset of wave instability.

It is proposed the wider layer ratio tolerance is attributed to increased stretching (extension) of the melt in the side stream prior to the stream joining the larger parallel stream. In this geometry, when the side stream joins with the main horizontal stream it is made to converge, and subsequently is subjected to extensional flow. The smaller height and increased velocity, leads to higher rates of extension in the melt. The extensional deformation results in an increased normal stress, which more closely matches the normal stress developed in melt of the parallel stream. Consequently the higher level of stretching leads to less imbalance in normal stress across the interface when the melt streams join.

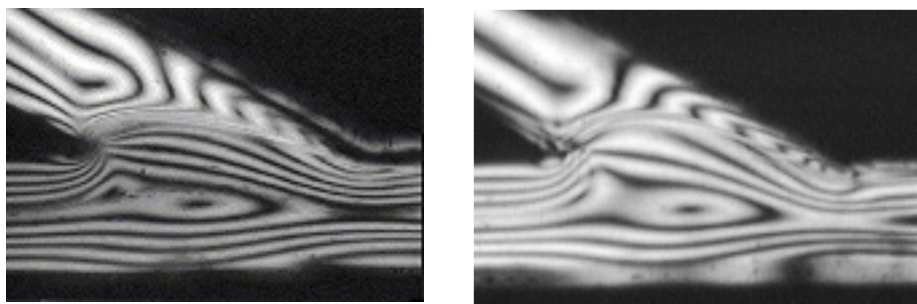
90° Die Geometries

Layer ratios resulting in wave type interfacial instability in this geometry are also summarised in Figure 5. Data is compared to those of the 30° geometry. Data for the Dow LD150R melt indicate the 90° geometry to be more stable than the 30° geometry with the 1.05 mm side stream height, but less stable when compared to 0.68 mm side stream geometry.

Extensional history of the melt streams appears to be the key factor affecting flow stability in this geometry. Flow stability is influenced by the level of pre-extension of melt in the perpendicular side channel before it joins the parallel stream. We have observed flow in the in the bottom channel influences the flow in the 0.83 mm high side stream of the 90° geometry upstream of the merging interface. The flow was observed to converge on approach to the end of the side stream in a similar fashion to the behaviour illustrated for the 30° geometry. Numerical simulation performed by a isothermal steady, two-dimensional, viscoelastic, finite element procedure to solve mass, momentum and energy conservation equations of melt flow in this geometry supports our proposition that contraction mechanisms improve flow stability in the 90° geometry.

Flow Analysis in Two Extruder Arrangement 2

The images presented in Figures 6(a) and 6(b) show the stress birefringence patterns obtained for the LDPE melt flow in the respective two extruder and single extruder arrangements. Apart from the differences in fringe order associated with the difference in flow rates in each arrangement there is found to be close similarity in pattern features. Wave type instability was again found to occur in the coextruded LDPE melt from this arrangement when processed under specific conditions. However, the stable processing window limits were found to be significantly wider compared to the bifurcated arrangement. For example, when the Dow LD150R melt was processed at 200°C and mass flow of 2.2 g.min⁻¹ on the dual extruder system the limits of the side/parallel stream layer ratios leading to wave type interfacial were < 0.157:1 and > 6.87:1. Lowering the melt temperature to 180°C and using the same mass flow rate results in a marginal reduction of the stable limits of the side-parallel stream layer ratios to < 0.16:1 and > 6.27:1. Interestingly, for this flow arrangement, the side- parallel and parallel-side ratios are almost equivalent for each flow rate. Overall, the dual extruder arrangement appears to promote more stable flow, allowing wider differences in layer ratios before the onset of wave instability, compared to the bifurcated arrangement at comparable flow rates. Studies were also conducted on Lupolen melt at 180°C at flow rate of approximately 2 g.min⁻¹. This study produced similar findings wherein side / parallel stream layer ratios resulting in interfacial instability were < 0.24:1 and > 5.6:1. Reducing the melt temperature to 140°C, thus increasing the melt elasticity, narrowed the range of stable flow layer ratio to between < 0.29:1 and > 4.84:1.



(a) (b)
FIGURE 6. Images of stress birefringence patterns of Dow LD150R melt flow in 30° die geometries. (a) two extruder arrangement, stable flow with 9 % mass flow in side channel, 3.06 g/min (b) single extruder same melt arrangement, 1.34 g/min 27 % mass flow in side channel with flow instability.

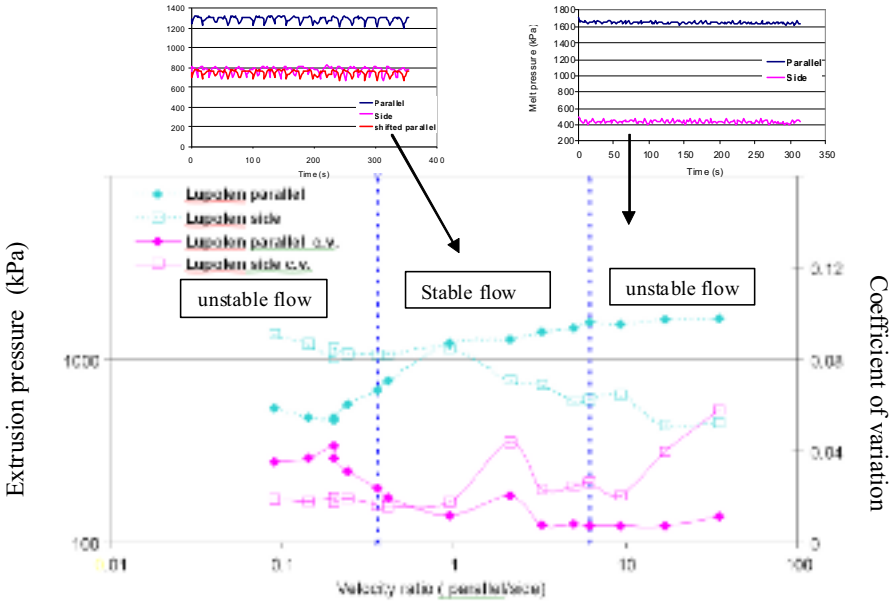
Frequency of Instability

We have found no evidence that would support the observed wave type interfacial instabilities being driven by temporal disturbances from extruder screw rotation. The birefringence pattern at immediate entry to the die land appeared stable in the Eulerian sense (the pattern appears static with time) during flow conditions that resulted in wave type interfacial instability in the extrudate.

A flow disturbance was however observed within the die land, especially near the die land exit. Image analysis was used to determine the plane at which the flow was most disturbed in Dow LD150R melt at a flow rate of 1.34 g.min⁻¹ in the bifurcated die for the side/parallel layer ratio of < 0.55:1, a condition giving rise to interfacial instability. More comprehensive details and the results of this particular study are given elsewhere [20]. The analysis revealed flow in the die land was most disturbed at a plane corresponding to 0.6 mm of the die land channel height which approximates to (0.6/1.07) ~ 0.56:1 proportion of the channel. This position was consistent with the measured interface position. Furthermore, the disturbance had temporal regularity. Fourier analysis was used to determine the periodicity of the change in grey scale at this plane. The time period of the disturbance was 0.85 s ~ 1.17 Hz. The extruder screw speed at this flow rate was 0.55 ± 0.002 rpm ~ 0.009 Hz. Clearly, the observed and measured periodicity of the instability does not correlate with harmonics of extruder screw noise.

The frequency of the wave disturbance in the Dow LD150R extrudate produced under these same processing conditions was evaluated by monitoring the change in grey scale of the extrudate surface. Fourier analysis of this data set indicated the periodicity of the extrudate surface disturbance to be 1.17 Hz, which is identical to the frequency of the disturbance noted in the melt flow in the die land. This consistency in disturbance frequency between die land melt flow and extrudate would suggest the instability arises in the die and that the wavenumber of the disturbance does not change as melt flow progresses along the die land. It should be noted

however that, to the eye, it was quite difficult to see any disturbance in the die land melt flow further upstream towards the confluent region suggesting that the wave amplitude grows with progress along the die. It is our belief that the instability is



initiated at the merging

FIGURE 7. Measured pressure (top images) and pressure variation during the coextrusion of Lupolen LDPE melt in the dual extruder arrangement.

point and not driven by pressure disturbances. Indeed, when we monitored pressure during conditions promoting stable and unstable flow in the dual extrusion system we found the contrary was true. We show, in Figure 7 that stable flow (no wave instability) occurred when stream pressure disturbances were at their greatest, and vice-versa.

Modelling

The flow of Dow LD150R melt at 200°C in the bifurcated die configuration was modelled at a mass flow rate of 1.34 g.min⁻¹.and there was found to be very good agreement between the modelling predicted zero shear stress and total stress loci contours and the experimentally determined 0° isoclinic loci. Typical modelled stress contours are shown in Figure 8. Although the modelled stress contours do not precisely match the location of experimentally measured stress contours, qualitatively there is good agreement in terms of the general shapes, profiles and concentrations of the measured and modelled total stresses. Modelling is demonstrated to be far superior

in terms of detailing the stress magnitudes. The modelling indicated much higher stresses are generated than can be interpreted by applying full-field optical techniques.

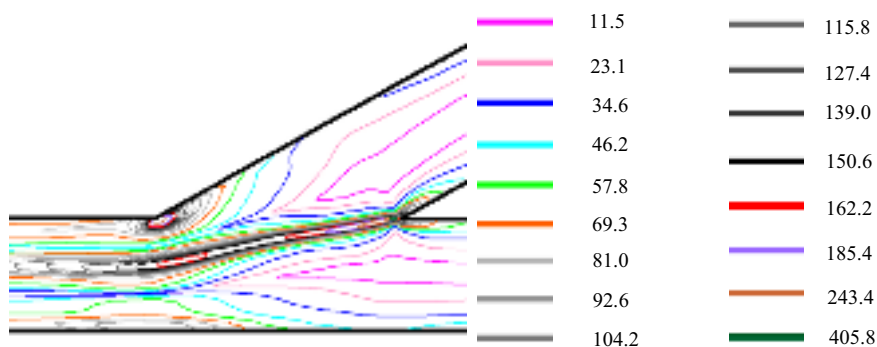


FIGURE 8. Modelled stress magnitude loci for Dow LD150R melt flow at a flow rate of 1.34 g/min. Values of isoclines in kPa.

The total normal stress difference (TNSD) criterion was used in the evaluation of the Dow LD150R melt at 200°C and flow rate 1.34 g.min⁻¹ in the bifurcated geometry. For the purposes of modelling it was assumed that all the channel dimensions were 1.0 mm. A series of side/parallel layer ratios close to and beyond those layer ratios producing interfacial instability were modelled. The particular flow conditions considered in the simulation are side/parallel layer ratio of approximately 0.62:1, 0.65:1 and 0.68:1. It was found the predicted TNSD profiles of each of these layer ratios remained positive along the whole length of the interface for the 0.65:1 and 0.68:1 conditions. By contrast, the TNSD profile changed sense, becoming negative for the 0.62:1 layer ratio at approximately 50 % along the interface length thus predicting interfacial instability at this layer ratio. This result was been found to be in good correspondence with the experimental data, i.e. predicted unstable layer ratio is 0.62:1 and the experimentally measured value is 0.55:1. Modelling conducted using the TNSD variable proved to be a useful tool for probing and understanding the mechanism(s) initiating the wave instability. The TNSD tool indicated that instability results from an imbalance in the total normal stress across the interface in the merging area as a consequence of melt in the minor stream being subject to the high extensional strain rate.

SUMMARY

The study conclusively shows it is possible for wave type interfacial instability to develop in coextruded melt streams of exactly the same melt. Hence, there does not necessarily need to be larger differences in melt stream rheology to drive the instability. Subtle changes in melt elasticity resulting from process history can drive the instability. Numerical simulations of the coextrusion process indicate the instability is driven by differences in the stretch histories of melts when forming

the interface. The differences in history lead to imbalance in the normal stress across the interface and this appears to initiate the instability. Simulations also suggest flow conditions that increase melt stretch in the side stream prior to entering the confluent region, either through increased stream velocity or forced convergence, promote stable flow in coextrusion. This hypothesis is supported by experimental work presented for the 30° and 90° geometries. Our study also demonstrates that the observed interfacial instability is that is initiated at the merging point and is not driven by pressure disturbances from the extruder screw.

ACKNOWLEDGMENTS

The financial support of IRC in Polymer Engineering and Bradford University and cooperation of Prof. M. Zatloukal, University of Zlín are gratefully acknowledged.

REFERENCES

1. S. Q. Wang, P. A. Drda and Y. W. Inn, *J. Rheol.* **40**, 875 (1996).
2. X. Yang, H. Ishida and S. Q. Wang, *J. Rheol.* **42**, 63 (1998).
3. N. El Kissi, J. M. Piau, *J. Rheol.* **38**, 1447 (1994).
4. T. J. Person and M. M. Denn, *J. Rheol.* **41**, 249 (1997).
5. T. C. Yu, C. D. Han, *J. Appl. Polym. Sci.* **17**, 1203 (1973).
6. A. Ya Malkin, M. L. Friedman, K. D. Vachagin, G. V. Vinogradov, *J. Appl. Polym. Sci.* **19**, 375 (1975).
7. C. D. Han and R. Shetty, *Polym. Eng. Sci.* **16(10)**, 697 (1976).
8. C. D. Han and R. Shetty, *Polym. Eng. Sci.* **18(3)**, 180 (1978).
9. C. D. Han and H. B. Chin, *Polym. Eng. Sci.* **19**, 1156 (1979).
10. W. J. Schrenk, N. L. Bradley, T. Alfrey and H. Maack, *Polym. Eng. Sci.* **18(8)**, 620 (1978).
11. H. Mavridis, A. N. Hrymak and J. Vlachopoulos, *AIChE J.* **33**, 410 (1987).
12. E. Mitsoulis and F. Heng, *J. Appl. Polym. Sci.* **34**, 1713 (1987).
13. R. Ramanathan and J. Dooley, *SPE ANTEC* **50**, 426 (1992).
14. S. Puissant, B. Vergnes, Y. Demay and J. F. Agassant, *Polym. Eng. Sci.* **32(3)**, 213 (1992).
15. R. Ramanathan and W. J. Schrenk, *Plast. Eng.* **6**, 73 (1993).
16. J. Dooley and B. T. Hilton, *SPE ANTEC* **51**, 3354 (1993).
17. M. T. Martyn, T. Gough, R. Spares and P.D. Coates, *SPE ANTEC* **59**, 1031 (2001).
18. M. T. Martyn, T. Gough, R. Spares, P.D. Coates and M. Zatloukal, *SPE ANTEC* **60**, (2002).
19. M. T. Martyn, T. Gough, R. Spares, P. D. Coates and M. Zatloukal, *SPE ANTEC* **62**, (2004).
20. M. T. Martyn, R. Spares, P. D. Coates and M. Zatloukal, *Plastics and Rubber Composites* **33**, 27-35 (2004).
21. M. Zatloukal, *J. Non-Newtonian Fluid Mech.* **113**, 209 (2003).

22. M. T. Martyn, R. Spares, P. D. Coates and M. Zatloukal. *J. Non-Newtonian Fluid Mech.* **156**, 150-164 (2009).
23. H. A. Barnes and G. P. Roberts, *J. Non-Newtonian Fluid Mech.* **44**, 113–126 (1992).
24. M. Zatloukal, J. Vlcek, C. Tzoganakis and P. Saha, *Int. Polym. Process.* **16(2)**, 198–207 (2001).
25. M. Zatloukal, J. Vlcek, C. Tzoganakis and P. Saha, *Polym. Eng. Sci.* **42(7)**, 1520–1533 (2002).

Copyright of AIP Conference Proceedings is the property of American Institute of Physics and its content may not be copied or emailed to multiple sites or posted to a listserv without the copyright holder's express written permission. However, users may print, download, or email articles for individual use.